Effect of neutron irradiation on hardening in MgO crystals

D. Cáceres, I. Vergara, and R. González
Departamento de Física, Escuela Politécnica Superior, Universidad Carlos III, Avenida de la Universidad, 30, 28911 Leganés, Madrid, Spain

Y. Chen
Division of Materials Sciences, Office of Basic Energy Sciences, SC 13, The US Department of Energy, Germantown, Maryland 20874-1290

(Received 10 January 2002; published 11 July 2002)

Using a nanoindentation technique, hardness and Young's modulus were determined in both nominally pure MgO and lithium-doped MgO crystals, before and after neutron irradiation in the dose range $10^{15}-10^{19}$ n/cm^2. The resulting defects were monitored by optical-absorption spectroscopy. The concentrations of single oxygen vacancies and higher-order point defects involving oxygen vacancies increase with neutron dose. A constant value of (290 ± 15) GPa for the Young's modulus was measured in all the crystals, indicating that the elastic properties are not influenced by either impurities or defects produced by irradiation. Hardness increases with neutron dose and is independent of the presence of lithium in the crystal. Neutron-irradiated crystals contain oxygen vacancies, higher-order point defects, and interstitials, whereas thermochemically reduced (TCR) crystals contain oxygen vacancies. Comparison between a neutron irradiated and a TCR MgO crystal containing similar concentrations of oxygen vacancies, shows that 70% of the hardening by neutron irradiation is produced by interstitials, 30% by oxygen vacancies, and a negligible amount by higher-order point defects.

DOI: 10.1103/PhysRevB.66.024111 PACS number(s): 61.72.Ji, 62.20.Qp, 62.20.Dc

I. INTRODUCTION

Ceramic oxides resistant to radiation damage are necessary for several important applications such as fission reactor fuel burnup, nuclear waste disposal, advanced energy systems such as fusion reactors, and electronic applications. It is known that radiation-induced defects generally increase both the lattice hardness and fracture stress. Identification of materials that can undergo high irradiation doses without a failure in the mechanical integrity is thus important.

Mechanical properties of magnesium oxide single crystals have been extensively studied using compression testing and microindentations.[1–17] Vacancies, interstitials, impurities, and their aggregates have been found to harden MgO crystals. As a result the flow stress strongly depends on the concentration of these defects.[1,2,8,11,14] Recently, nanoindentation experiments have been performed in MgO single crystals to study the low stress plasticity[18–23] and pop-in phenomenon.[19,24]

Some of the important features of the present study are as follows.

(1) Nanoindentation is a unique and versatile technique for studying the mechanical properties of bulk materials and films. Because nanoindentation is a nondestructive technique, measurements can be performed on *the same* sample. In measuring thermal annealing effects, only one sample is needed to obtain the statistical average of the mechanical parameters for different annealing temperatures.

(2) Comparison between neutron-irradiated crystals and thermochemically reduced (TCR) crystals. The former contain anion vacancies, higher-order point defects involving oxygen vacancies, and oxygen interstitials. TCR crystals are produced under stringent conditions that yield nonstoichiometric deficiency of oxygen ions, and therefore contain primarily oxygen vacancies, virtually free of interstitials and higher-order point defects involving oxygen vacancies.

(3) Nanoindentation measures hardness and Young's modulus. Compression tests measure flow stress.

(4) To explore the effect of a light-ion impurity as a result of neutron irradiation. The intended impurity was lithium, which has a strong affinity for hydrogen. Therefore, lithium-doped MgO crystals contain large concentrations of both lithium and hydrogen. An added incentive to study this system is that it has been reported that lithium-doping resulted in suppression of oxygen-vacancy formation.[25,26]

II. EXPERIMENTAL PROCEDURE

The MgO crystals used in this investigation were grown at the Oak Ridge National Laboratory by an arc-fusion technique using high-purity MgO powder from Kanto Chemical Chemistry, Tokyo, Japan.[27] Lithium doping was achieved by mixing 5% of Li_2CO_3 powder with MgO powder before crystal growth. The actual lithium concentration in the resulting single crystals was determined by spectrographic analysis to be about 400 ppm. Single-crystal specimens having {100} faces were cleaved from ingots in the boule.

Neutron irradiations were performed either at the Oak Ridge National Laboratory, Low Temperature Neutron Irradiation Facility or at the High Flux Reactor of the Institute for Advanced Materials of the Joint Research Center at Petten using fluxes of 2.0×10^{17} and 7.8×10^{17} fission spectrum n/cm^2 s ($E>0.1$ MeV), respectively. The ambient temperature was in both cases 325 ± 20 K.

TCR was performed at $T\sim2300$ K under 7 atm of Mg vapor. The result was a nonstoichiometric deficiency of oxy-

gen ions, an absence of interstitials, and virtually no higher-order point defects. However, under extreme TCR conditions, small amounts of oxygen divacancies can be expected and observed. Divacancies are formed statistically when the oxygen-vacancy concentration is sufficiently large.

Optical-absorption measurements in the UV-VIS-IR (ultra voilet-visible-infrared) regions were made with a Perkin-Elmer Lambda 19 spectrophotometer. Far-infrared data were taken with a Perkin-Elmer FT-IR 2000 spectrophotometer. Heat treatments were made in flowing high-purity nitrogen gas inside a horizontal furnace.

The nanoindenter continuously measures the load and displacement of a three-sided pyramidal diamond indenter as it is pushed into the sample. Hardness is obtained as a function of indent depth during loading by dividing the applied load by the projected area of the indenter tip. The elastic modulus is derived from the slope of the load-displacement curve upon unloading as the material recovers elastically.[28]

Nanoindentation experiments were made with a Nanoindenter IIs (Nano Instruments, Inc., Knoxville, TN) mechanical properties microprobe. All tests were performed at room temperature. Each specimen was tested using the continuous stiffness measurement technique developed by Pethica and Oliver.[29] This technique enables continuous measurement of the stiffness and the area of contact between the indenter and the specimen during indentation. To measure the contact stiffness continuously during an indentation, a very small ac current of known frequency is superposed on the load coil of the indenter. This current, which is much smaller than the dc current that determines the nominal load on the indenter, causes the indenter to oscillate with a displacement amplitude and phase shift related to the stiffness of the contact area. A comparison of the phase and amplitude of the indenter oscillations (determined with a two-phase lock-in amplifier) with the phase and amplitude of the imposed ac signal allows the stiffness to be calculated either in terms of amplitude or phase. The contact stiffness, applied load and indenter displacement can then be used to determine the mechanical properties as a function of the indenter depth.

The samples were polished with diamond paste from Struers and the grain size was 3 μm. A good quality of the sample surface is essential for accurate and reproducible data. For all the tests, care was taken throughout to establish maximum thermal stability of the sample prior to testing. The thermal drift was less than 0.05 nm/s. An average of ten indents were made in each specimen. Hardness and Young's modulus values were obtained by averaging the results for all indents at a penetration depth of 1000 nm.

III. EXPERIMENTAL RESULTS

A. Defect characterization

Optical absorption was used to characterize the defects incurred in the reactor. The well-characterized defects are (1) oxygen vacancies (primarily the one-electron F^+ center) which absorb at 252 nm (4.92 eV),[30,31] (2) oxygen divacancies F_2, which absorb at 355 and 975 nm (3.49 and 1.27 eV, respectively),[32–35] and (3) an unidentified defect that absorbs at 572 nm (2.16 eV).[30,35–38] Cations are also displaced, but quickly combine with the vacancies.

TABLE I. Neutron doses for seven undoped and four Li-doped MgO crystals.

Sample	Dose(n/cm^2)
MgO(1)	5.3×10^{15}
MgO(2)	2.0×10^{16}
MgO(3)	6.4×10^{16}
MgO(4)	1.0×10^{17}
MgO(5)	1.1×10^{18}
MgO(6)	2.4×10^{18}
MgO(7)	6.9×10^{18}
MgO:Li(1)	1.0×10^{17}
MgO:Li(2)	2.2×10^{17}
MgO:Li(3)	1.0×10^{18}
MgO:Li(4)	1.0×10^{19}

Seven nominally pure and four Li-doped MgO crystals were neutron irradiated to different doses, as shown in Table I. After neutron irradiation, the most intense band occurs at 252 nm, which has been attributed mostly to F^+ centers.[39] (Both the two-electron F center and the one-electron F^+ center absorb at about this wavelength. Therefore this band can be considered as due to oxygen vacancies.) The concentration of oxygen vacancies increases with neutron dose. Other observed bands, associated with higher-order point defects, are F_2 at 355 and 975 nm; and the defects absorbing at 572 nm.[36]

Figure 1 shows the optical-absorption spectra of undoped MgO crystals irradiated to doses between 5.3×10^{15} n/cm^2 and 6.9×10^{18} n/cm^2, which went slightly beyond the dose range performed by Chen *et al.*[35] (their samples were irradiated up to a dose of 5.4×10^{18} n/cm^2). The optical characteristics and annealing behavior were essentially the same in both studies. The 572-nm band grows disproportionately

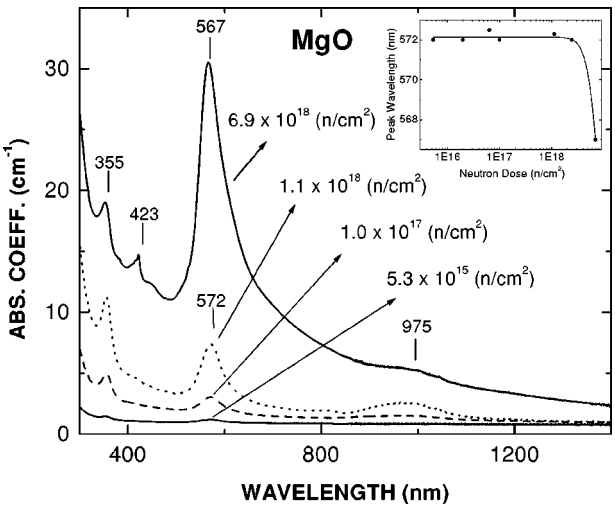

FIG. 1. Optical-absorption spectra of MgO crystals irradiated to different neutron doses. The inset shows the peak position of the absorption band at 572 nm vs irradiation dose for MgO crystals.

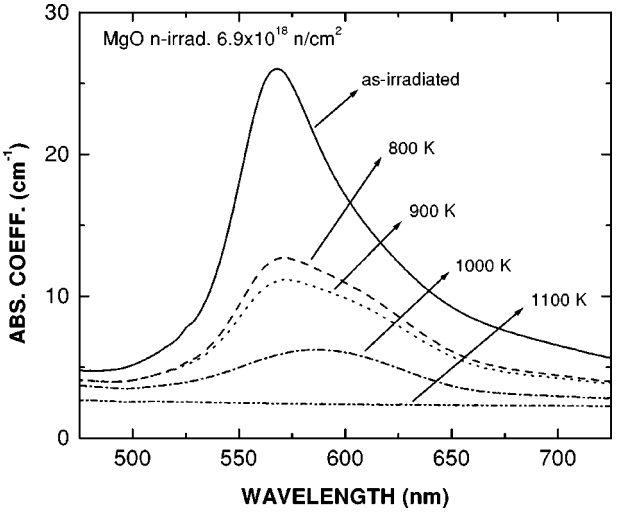

FIG. 2. Optical-absorption spectra of the 572-nm band in MgO (7) crystal after isochronal annealing for 15 min at several selected temperatures.

faster than the F_2 bands with increasing neutron dose. Upon isochronal annealing at increasing temperatures, the peak consistently shifted to lower wavelengths, from 572 to 565 nm.[37,38] The dose at 6.9×10^{18} n/cm^2 yielded two departing observations. First, the peak occurs at 567 nm instead of 572 nm (Fig. 1 inset). Second, the peak at 567 nm shifts to higher wavelengths with annealing (Fig. 2).

The counterpart spectra of irradiated MgO:Li crystals are shown in Fig. 3. The most striking difference between these spectra and those of the undoped crystals is that at doses below 1×10^{18} n/cm^2, the concentration of higher-order point defects (monitored by the absorption at 355, 416, 423, 572, and 975 nm) and the oxygen-vacancy concentration, as determined by the absorption at 252 nm (not shown in the figure), was much lower in MgO:Li samples, confirming previous findings.[25,26] Recently, this suppression of oxygen vacancies has been attributed to oxygen vacancies camouflaging as $[H^-]^+$ centers (an oxygen vacancy with two electrons

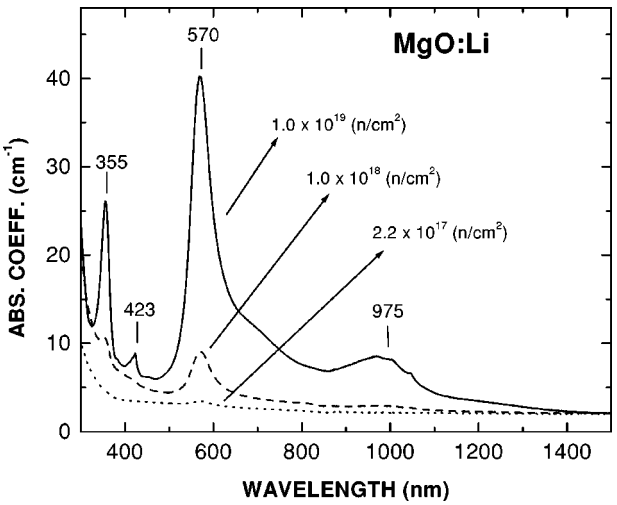

FIG. 3. Optical-absorption spectra of MgO:Li crystals irradiated to different neutron doses.

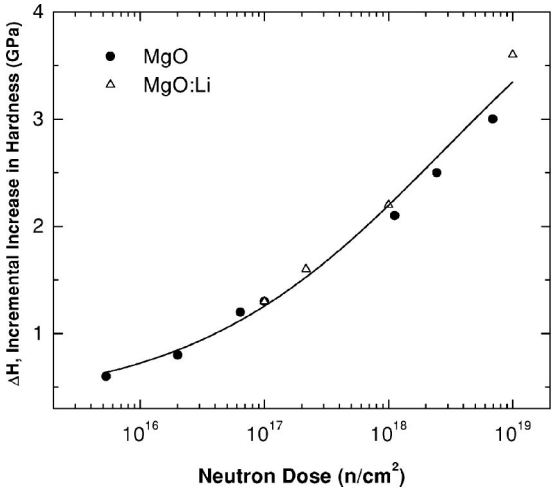

FIG. 4. The incremental increase in hardness ΔH against neutron dose for MgO and MgO:Li crystals.

occupied by a proton and therefore positively charged relative to the lattice).[26] The neutral oxygen vacancy had simply captured a proton, and the optical absorption reflected a local-mode vibration instead.

B. Nanoindentation measurements

Nanoindentation experiments were performed in both as-grown MgO and MgO:Li crystals, before and after neutron irradiation. A constant value of (290 ± 15) GPa for the Young's modulus was obtained in both types of crystals, in agreement with earlier results.[40] Before irradiation, both types of crystals showed a hardness value of (9.1 ± 0.2) GPa. Hardness increased with dose. At the highest dose of 1.0×10^{19} n/cm^2, hardness reached 12.9 ± 0.3 GPa in a MgO:Li crystal. The increment in hardness ΔH, which represents the difference between an irradiated and an unirradiated crystal, is shown in Fig. 4. We conclude that ΔH is independent of the presence of lithium impurities and increases with neutron dose.

Hardening of neutron-irradiated MgO crystals has been previously investigated by flow stress in compression testing and microindentation experiments. The observed radiation hardening was attributed to interstitial-type defects.[1,2] To assess the role played by interstitials, a comparison of ΔH is made between a neutron-irradiated MgO sample and a TCR MgO crystal containing comparable amounts of oxygen vacancies, 3.4×10^{18} cm^{-3} and 4×10^{18} cm^{-3}, respectively. The neutron-irradiated crystal was irradiated to 6.9×10^{18} n/cm^2. (The TCR sample was also used in Ref. 40.) Both types of crystals have an abundance of oxygen vacancies, as monitored by the absorption band at 252 nm. The difference is that whereas neutron-irradiated crystals contain an abundance of interstitials and higher-order point defects, TCR crystals are virtually free of these defects.

The result is that ΔH for the neutron-irradiated crystal was significantly larger than that of the TCR crystal, 3.0 GPa and 1 GPa, respectively. It is therefore reasonable to conclude that the enhanced hardness is mostly due to interstitials and/or higher-order point defects, such as divacancies.

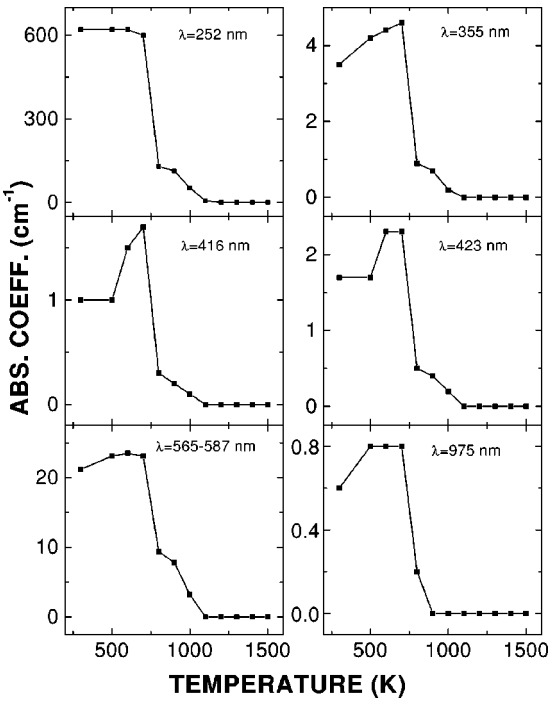

FIG. 5. Absorption coefficient versus annealing temperature for several absorption peaks in MgO(7).

However, based on the discussion in Sec. IV, higher-order point defects can be ruled out as important contributors to hardness.

C. Radiation recovery in neutron-irradiated samples

An MgO and MgO:Li sample irradiated up to doses of 6.9×10^{18} n/cm^2 and 1.0×10^{19} n/cm^2, respectively, were isochronally annnealed at increasing temperatures above 500 K in flowing nitrogen gas. After each anneal both the optical-absorption spectra and hardness were measured at room temperature.

1. Undoped MgO crystals

The absorption coefficients of several optical peaks are plotted in Fig. 5 as a function of annealing temperature. The most intense band was at 252 nm. The major annealing stage occurred between 700 and 800 K for all the bands. By 1000 K most of the bands had virtually disappeared. After the anneal at 1100 K, a band at about 217 nm was resolved. Its full width at half maximum (FWHM) was 0.53 eV. This band appears to be the same as the one observed in deformed MgO crystals with a FWHM of 0.6 eV.[4] The defect responsible for this absorption has not been identified. These results indicate that annealing of neutron-irradiated crystals results in the same defect produced by plastic deformation. At 1500 K the deformation band vanishes.

Figure 6 shows the recovery of ΔH versus the anneal temperature. ΔH remains practically constant until 1000 K and decreases very rapidly at higher temperatures. By 1400 K, ΔH becomes negligible, indicating that the preirradiation hardness has been restored.

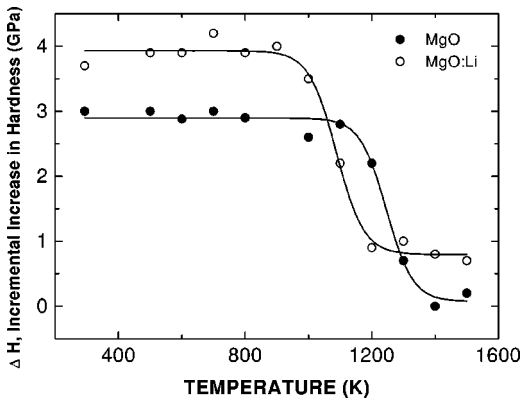

FIG. 6. The incremental increase in hardness versus isochronal annealing temperature for MgO(7), and MgO:Li(4).

2. Li-doped MgO crystals

The behavior of the bands produced by irradiation when the MgO:Li crystal is subjected to isochronal anneals at increasing temperatures is similar to the one already described for the undoped crystal. However, two observations are noted. First, after the anneal at 700 K an IR band at 1024 cm^{-1} starts to develop. This band has been previously attributed to $[H^-]^+$ centers.[41,42] This observation indicates that oxygen vacancies camouflage as $[H^-]^+$ centers.[26] The evolution of the intensity of this band during the thermal anneals is summarized in Fig. 7. It reaches a maximum at about 900 K, and completely vanishes by 1200 K. Second, after the anneal at 1100 K the band at 217 nm is absent; instead a band at about 235 nm is resolved. The latter band has been previously observed in MgO:Li crystals annealed at temperatures above 1400 K. The defect responsible for this band is probably related to the association of substitutional lithium ions and oxygen vacancies.[43,44]

The recovery of ΔH versus the anneal temperature is shown in Fig. 6. These results are qualitatively the same as those for the undoped crystal. The most noticeable difference occurs at the highest temperatures; while ΔH approaches to zero in the undoped crystal, the minimum value for ΔH in

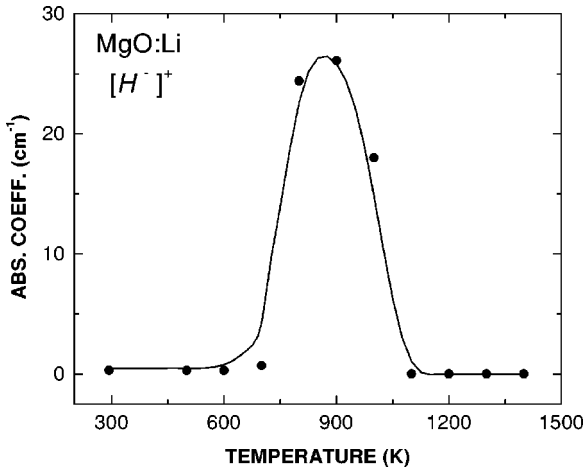

FIG. 7. Absorption coefficient of the $[H^-]^+$ center band versus isochronal annealing temperature for MgO:Li(4).

MgO:Li is ~ 0.8 GPa. This value is due to the emergence of an absorption band at 690 nm, associated with the presence of $[Li]^0$ centers. The linear configuration of this defect is Mg^{2+}-O^{2-}-Li^{+}-O^{-}, where O^{-} refers to an oxygen ion with a trapped hole.[45,46] The 690-nm band has been previously observed in MgO:Li crystals oxidized at temperatures above 1100 K. Our experiments were performed in nitrogen gas with some residual oxygen content. An increase in hardness in MgO:Li after oxidation has been reported earlier.[40]

IV. DISCUSSION

We shall now estimate the contributions of the three components (oxygen vacancies, higher-order point defects, and interstitials) in neutron-irradiated crystals to ΔH. As noted above, neutron-irradiated crystals contain oxygen vacancies, higher-order point defects involving oxygen vacancies, and oxygen interstitials. On the other hand, thermochemically reduced crystals contain oxygen vacancies and virtually none of the others. For the MgO crystal irradiated to a dose of 6.9×10^{18} n/cm^2, the oxygen-vacancy concentration was 3.4×10^{18} cm^{-3} and ΔH was 3.0 GPa. For the TCR crystal with comparable oxygen vacancies (4×10^{18} cm^{-3}), ΔH was 1.0 GPa. This indicates that in the neutron-irradiated crystal the contribution of oxygen vacancies to ΔH was about 30%. To estimate ΔH for higher-order point defects relative to that of oxygen vacancies, we obtain the ratio of the areas under the curves for the 355-, 572-, and 975-nm bands to that of the 252-nm band when plotted on photon energy scale. The ratio is ~ 0.01. Therefore the contributions of the higher-order point defects to ΔH is negligible. The errors will be small, even if the oscillators strengths of the bands are appreciably smaller than unit, or that the 355- and 975-nm bands are electronic transitions from the same defect.[33] This leaves $\Delta H = 2.0$ GPa from interstitials. We conclude that the major contributor to hardness in neutron-irradiated MgO crystals is interstitials.

Analyzing the annealing behavior, from Fig. 6, we note that annealing at 1100 K resulted in loss of hardness, corresponding to $\Delta H = -0.2$ GPa. At this temperature the bands at 252, 355, 416, 423, 572, and 975 nm were thermally destroyed (Fig. 5). Therefore we would expect a loss corresponding to $\Delta H = -1.0$ GPa from these six bands, and from a fraction of the $\Delta H = 2.0$ GPa from interstitials recombining with these bands. Such a large variation of ΔH was not observed at 1100 K, (Fig. 6), which can be accounted for by the emergence of the 217-nm band.

Concerning the suppression of the 252-nm band in MgO:Li, we note that ΔH is unaffected by the presence of lithium (Fig. 4). This result suggests that the concentration of oxygen interstitials, and to a lesser extent, oxygen vacancies and higher-order defects, is the same in MgO and MgO:Li. Hence the loss of oxygen vacancies observed at neutron doses below 10^{18} n/cm^2 is unlikely to be due to the lack of oxygen interstitials. This interpretation is compatible with our finding that protons were trapped by oxygen vacancies, thereby camouflaging oxygen vacancies as $[H^-]^+$ centers.

V. SUMMARY AND CONCLUSIONS

Oxygen vacancies, oxygen divacancies, and a defect(s) absorbing at 572 nm were spectroscopically characterized in nominally pure and lithium-doped MgO in the dose range of $10^{15}-10^{19}$ neutrons/cm^2 by optical absorption. In MgO:Li crystals irradiated with neutron doses below 10^{18} n/cm^2, hardness measurements confirm that most of the oxygen vacancies are camouflaged as $[H^-]^+$ centers.[26]

Young's modulus and hardness were determined by a nanoindentation technique. A constant value of (290 ± 15) GPa for the Young's modulus was measured in all the crystals, indicating that the elastic properties are not influenced by either lithium or intrinsic defects produced by irradiation. As-grown crystals show a hardness value of (9.1 ± 0.2) GPa. The incremental increase in hardness with dose is independent of the presence of Li ions.

A comparison of the incremental increase in hardness ΔH of a neutron-irradiated MgO crystal with a thermochemically reduced MgO crystal, which contained only oxygen vacancies, reveals that 70% of ΔH is contributed by oxygen interstitials and 30% by oxygen vacancies; higher-order point defects make a negligible contribution.

ACKNOWLEDGMENTS

Research at the University Carlos III was supported by the CICYT of Spain. The research of Y.C. is an outgrowth of past investigations performed at the Solid State Division of the Oak Ridge National Laboratory. The irradiation at the High Flux Reactor of the Institute for Advanced Materials of the Joint Research Center (JRC) at Petten was carried out under Contract No. 40.00024 with the European Atomic Energy Commission.

[1] R.W. Davidge, J. Nucl. Mater. **25**, 75 (1968).
[2] W.C. McGowan and W.A. Sibley, Philos. Mag. **19**, 161 (1969).
[3] M. Srinivasan and T.G. Stoebe, J. Mater. Sci. **9**, 121 (1974).
[4] Y. Chen, M.M. Abraham, T.J. Turner, and C.M. Nelson, Philos. Mag. **32**, 99 (1975).
[5] A.G. Evans and T.G. Langdon, Prog. Mater. Sci. **21**, 171 (1976).
[6] R.D. Newton and W.A. Sibley, Phys. Status Solidi A **41**, 569 (1977).
[7] R. W. Davidge, *Mechanical Behaviour of Ceramics* (Cambridge University Press, Cambridge, 1979).
[8] V.M. Orera, Phys. Status Solidi A **65**, 293 (1981)
[9] R. González, J. Piqueras, and J. Llopis, J. Appl. Phys. **53**, 7534 (1982).
[10] W.R. Cannon and T.G. Langdon, J. Mater. Sci. **18**, 1 (1983).
[11] J. Narayan and Y. Chen, Philos. Mag. A **49**, 475 (1984).
[12] K.S. Ramesh, E. Yasuda, S. Kimura, and K. Urabe, J. Mater. Sci. **21**, 4015 (1986).
[13] K.S. Ramesh, E. Yasuda, S. Kimura, J. Mater. Sci. **21**, 3147 (1986).

[14] J. Narayan, Y. Chen, and K.L. Tsang, Philos. Mag. A **55**, 807 (1987).
[15] K.C. Goretta and J.L. Routbort, J. Mater. Sci. Lett. **6**, 862 (1987).
[16] M. Srinivasan and T.G. Stoebe, J. Appl. Phys. **41**, 3726 (1970).
[17] R.W. Davidge, J. Mater. Sci. **2**, 339 (1967).
[18] M.Y. Khan, L.M. Brown, and M.M. Chaudhri, J. Phys. D **25**, A257 (1992).
[19] J. Woirgard, C. Tromas, J.C. Girard, and V. Audurier, J. Eur. Ceram. Soc. **18**, 2297 (1998).
[20] K. Sangwal, P. Gorostiza, and F. Sanz, Surf. Sci. **442**, 161 (1999).
[21] C. Tromas, J.C. Girard, V. Audurier, and J. Woirgard, J. Mater. Sci. **34**, 5337 (1999).
[22] K. Sangwal, P. Gorostiza, and F. Sanz, Surf. Sci. **446**, 314 (2000).
[23] C. Tromas, J.C. Girard, and J. Woirgard, Philos. Mag. A **80**, 2237 (2000).
[24] C. Tromas, J. Colin, C. Coupeau, J.C. Girard, J. Woirgard, and J. Grilhé, Eur. Phys. J.: Appl. Phys. **8**, 123 (1999).
[25] Y. Chen and M.M. Abraham, J. Am. Ceram. Soc. **59**, 101 (1976).
[26] R. González, I. Vergara, D. Cáceres, and Y. Chen, Phys. Rev. B **65**, 224108 (2002).
[27] M.M. Abraham, C.T. Butler, and Y. Chen, J. Chem. Phys. **55**, 3752 (1971).
[28] W.C. Oliver and G.M. Pharr, J. Mater. Res. **7–6**, 1564 (1992).
[29] J.B. Pethica and W.C. Oliver, Mater. Res. Soc. Symp. Proc. **130**, 13 (1989).
[30] Y. Chen, J.L. Kolopus, and W.A. Sibley, Phys. Rev. **186**, 865 (1969).
[31] L.A. Kappers, R.L. Kroes, and E.B. Hensley, Phys. Rev. B **1**, 4151 (1970).
[32] I.K. Ludlow and W.A. Runciman, Proc. Phys. Soc. London **86**, 1081 (1965).
[33] I.K. Ludlow, Proc. Phys. Soc. London **88**, 763 (1966).
[34] B. Henderson and J.E. Wertz, Adv. Phys. **17**, 749 (1968).
[35] Y. Chen, R.T. Williams, and W.A. Sibley, Phys. Rev. B **182**, 960 (1969).
[36] B. Henderson and R.D. King, Philos. Mag. **13**, 1149 (1966).
[37] Y. Chen and W.A. Sibley, Philos. Mag. **20**, 217 (1969).
[38] R. González, Y. Chen, R.M. Sebeck, G.P. Williams, Jr., R.T. Williams, and W. Gellermann, Phys. Rev. B **43**, 5228 (1991).
[39] W.A. Sibley and Y. Chen, Phys. Rev. **160**, 712 (1967).
[40] D. Cáceres, I. Vergara, R. González, and Y. Chen, Philos. Mag. A **82**, 1159 (2002).
[41] R. González, Y. Chen, and M. Mostoller, Phys. Rev. B **24**, 6862 (1981).
[42] R. González, R. Pareja, and Y. Chen, Phys. Rev. B **45**, 12 730 (1992).
[43] J.B. Lacy, M.M. Abraham, J.L. Boldú, Y. Chen, J. Narayan, and H.T. Tohver, Phys. Rev. B **18**, 4136 (1978).
[44] V.M. Orera, Y. Chen, and M.M. Abraham, Philos. Mag. A **41**, 431 (1980).
[45] J. Narayan, M.M. Abraham, Y. Chen, and H.T. Tohver, Philos. Mag. A **37**, 909 (1978).
[46] M.M. Abraham, Y. Chen, L.A. Boatner, and R.W. Reynolds, Phys. Rev. Lett. **37**, 849 (1976).